



Deposited via The University of Sheffield.

White Rose Research Online URL for this paper:

<https://eprints.whiterose.ac.uk/id/eprint/200990/>

Version: Accepted Version

Article:

Boatwright, S., Mounce, S., Romano, M. et al. (2023) Integrated sensor placement and leak localization using geospatial genetic algorithms. *Journal of Water Resources Planning and Management*, 149 (9). ISSN: 0733-9496

<https://doi.org/10.1061/jwrmd5.wreng-6037>

This material may be downloaded for personal use only. Any other use requires prior permission of the American Society of Civil Engineers. This material may be found at <https://doi.org/10.1061/JWRMD5.WRENG-6037>

Reuse

Items deposited in White Rose Research Online are protected by copyright, with all rights reserved unless indicated otherwise. They may be downloaded and/or printed for private study, or other acts as permitted by national copyright laws. The publisher or other rights holders may allow further reproduction and re-use of the full text version. This is indicated by the licence information on the White Rose Research Online record for the item.

Takedown

If you consider content in White Rose Research Online to be in breach of UK law, please notify us by emailing eprints@whiterose.ac.uk including the URL of the record and the reason for the withdrawal request.

1 INTEGRATED SENSOR PLACEMENT AND LEAK LOCALISATION USING GEOSPATIAL GENETIC
2 ALGORITHMS

3 ¹Shaun Boatwright, ²Stephen Mounce, ³Michele Romano and ⁴Joby Boxall.

4 ¹ Affiliation: Department of Civil and Structural Engineering, University of Sheffield, Sheffield, S1
5 3JD, UK. Email: Shaun.Boatwright@sheffield.gov.uk

6 ² Affiliation: Department of Civil and Structural Engineering, University of Sheffield, Sheffield, S1
7 3JD, UK. Email: s.r.mounce@sheffield.ac.uk (Corresponding Author)

8 ³ Affiliation: Data and Analytics Team, United Utilities Water Limited, Warrington, WA5 3LP, UK.E-
9 mail: Michele.Romano@uuplc.co.uk

10 ⁴ Affiliation: Department of Civil and Structural Engineering, University of Sheffield, Sheffield, S1
11 3JD, UK. Email: J.B.Boxall@sheffield.ac.uk

12

13 **ABSTRACT**

14 There is an urgent need to reduce water loss from drinking water distribution systems. A
15 novel framework that integrates the placement of multiple pressure sensor and localisation
16 using geospatial techniques is developed and validated to find leaks/bursts as they occur
17 within District Meter Areas (DMA). A data-driven leak/burst localisation technique, featuring
18 a novel spatially constrained inverse-distance weighted interpolation technique, was
19 developed which quantifies the change in pressure due to a new leak/burst event using
20 pressure sensors deployed in a DMA. The integrated framework uses the same modelling
21 results and geospatial search techniques in both the optimal sensor placement and leak/burst
22 localisation steps. It can be adapted for any data-driven or model-based leak/burst localisation
23 technique and is not dependent on high hydraulic model calibration requirements such as
24 high density smart meter deployment. Validation is presented using data from 16 engineered

25 events (field work flushing) conducted in an operational DMA. Results show good agreement
26 between the leak/burst localisation performance for real and modelled engineered events
27 demonstrating that the sensor placement technique can accurately predict the expected
28 performance of an operational DMA. This is particularly the case as the number of optimal
29 sensors increases. Engineered events as small as 3.5% of the peak daily flow (6% of the
30 average daily flow) were correctly localised with search areas containing as few as 14% of
31 the pipes in the DMA (using only four pressure sensors).

32

33 **Key words:** Leak/burst localisation, optimal sensor placement, evolutionary algorithm,
34 spatial constraint, network analysis, field testing

35 **INTRODUCTION**

36 The size and capacity of a water distribution system (WDS) is dictated by the demographics
37 of the supplied area and the distance between the source and the served population. In the
38 Western world these are generally large, complex (and often ageing) infrastructures and
39 water is inevitably lost between the points of treatment and consumption. Failures such as
40 leak and burst events are a serious problem because they disturb customer supplies, lead to
41 water loss (with subsequent impacts on cost, energy and carbon footprint), can lead to
42 potential contamination and managing and repairing them consumes vast resources (Colombo
43 and Karney, 2002, Fox et al. 2016). These various factors combine so that that water utilities
44 need to develop new solutions and methods to better target the collection of data and its
45 analysis, in order to decide where money should be invested to efficiently and effectively
46 reduce water loss.

47 Much leakage management is reactive consisting of activities to detect, localise and repair
48 leaks once they have occurred so as to minimise the impact on customers and the associated
49 water loss. A district metered area (DMA) is a sub-section of the network which is partially
50 hydraulically isolated from the surrounding network and flow is monitored at all entry and
51 exit points. Detection aims to confirm the presence of leakage events and, where DMAs have
52 been implemented, to provide an approximate location so that targeted intervention can be
53 undertaken to resolve the problem quickly and with minimal disruption to customers. The
54 current level of WDS monitoring makes detection (i.e. identifying the DMA(s) containing
55 leak events) possible but localisation (or narrowing down the area within a DMA containing
56 the event) requires a higher density of sensors than are currently deployed in most WDSs
57 (Mounce et al. 2010, Xu et al. 2020). Most pressure sensors can be installed using a pressure
58 tapping which means that access to only a portion of the pipe is required (and / or fire
59 hydrants can be used) as opposed to flow sensors which require total excavation and pipe
60 isolation.

61 Often, water companies are still typically reliant on their customers reporting problems with
62 the water supply (such as low pressure / no water or a visible event) and on the use of labour
63 intensive and expensive manual acoustic techniques. A number of modern techniques are
64 currently used to allow the assessment, detection and control of leaks within WDS. Previous
65 reviews by Puust et al. (2010) and Mutikanga et al. (2013) cover the range of various
66 techniques and how they can be classified.

67 Engineered events are physically simulated flushing events introduced into a WDS by
68 opening fire hydrants in the field and are used because they allow the run time, location and
69 size of the event to be controlled. Determining the most informative size of leak or burst
70 events to model represents a significant challenge. Large events typically impact the supplies

71 of customers and must be dealt with swiftly to reduce the impact on targets related to
72 customer supplies. Smaller events tend to be more difficult to detect and localise. There are a
73 range of intermediate event sizes which are both too small to be readily apparent but also
74 large enough to be localised using additional sensors placed throughout a DMA (referred to
75 here as leak/ bursts).

76 This paper presents the details of a novel methodological framework for approximate
77 leak/burst location. It encompasses a method for selecting the optimal number and location of
78 sensors to be deployed in a particular DMA in order to achieve a desired level of event
79 location performance whilst minimising the dependency on accurate hydraulic models. This
80 is a significant advance on sensor placement techniques which only use spacing or entropy
81 (in the sense of information theory) to determine the optimal configurations. This tight
82 coupling between optimal sensor placement and approximate burst/leak location is of
83 particular importance as an optimal sensor placement strategy depends on the method that is
84 used to locate the potential leaks/bursts and likewise the efficiency of the burst/leak location
85 depends on the sensor placement. Multiple engineered events (via field work) are used to
86 validate the framework of methods.

87

88 **LITERATURE REVIEW**

89 As part of the transition to smart networks, continuous, near real-time monitoring of WDS's
90 hydraulic parameters (i.e. pressure and flow) has been the focus of significant research and
91 development. Automatic near real-time techniques have been developed and implemented to
92 minimise the leak/burst awareness time (Mounce et al. 2010, Romano et al. 2014) by
93 effectively detecting, at the DMA level, leaks/bursts as soon as they occur (Li et al. 2015). A

94 wide range of innovative data-driven leak/burst detection techniques utilising machine
95 learning and advanced statistical tools have been developed (including with the use of deep
96 learning, as in Wang et al. (2020)) which can analyse the large amounts of data and some
97 have been implemented by water utilities (Wu and Liu, 2017), with wider proliferation
98 ongoing as sensor rollout continues. After it is established that an event has occurred in a
99 DMA, the next challenge is to determine the exact event location. Pressure data can help
100 locate bursts when the pressure meters are properly deployed in a DMA, the temporal varying
101 correlation of pressure drops between data from several pressure sensors in a single DMA
102 providing a fingerprint to help with localization (Wu et al. 2018). This is challenging due to
103 the often limited numbers of available pressure sensors within a DMA. The latest trends for
104 leak/burst localisation pressure sensor deployment show that sensor densities of fewer than
105 five pressure sensors per DMA are commonly deployed in the real world (Soldevila et al.
106 2019). Daniel et al. (2023) presented a pressure-driven algorithm for leakage identification
107 and localization. Time series pressure data was used for leakage detection, with the sensor
108 closest to the leak pinpointed and then this being utilized for localization via a hydraulic
109 model (requiring a demand-calibrated model with smart meter data). Whilst the technique
110 was able to localize leakages with an average distance of 149m in the case study presented,
111 requirements included an almost error-free pressure calibrated model, 33 pressure sensors
112 over 3 DMAs and demand data from 82 smart meters. Steffelbauer et al. (2022) tackled the
113 same case study (BattLeDIM) with a method which consists of calibrating the nodal demand
114 and pipe roughness and introducing a dual model for the calibrated primal problem to detect
115 and locate leaks. They note that data set contains an unrealistically high number of sensors.

116 Methods which utilise hydraulic data to determine the approximate location of leaks and
117 bursts within a DMA have emerged (Casillas et al. 2013a, Farley et al. 2013, Romano et al.

118 2013, Boatwright et al. 2016). In general these methods are not integrated with the detection
119 step. These methods can allow a further reduction in the response time to leak/burst events by
120 providing an indication of their likely location as a prelude to finding their precise location
121 (i.e., pinpointing on a pipe). Key to the success of these approximate leak/burst location
122 methods is the placement of the additional instrumentation.

123 As only a limited number of sensors can be installed in WDSs due to budget constraints and
124 since improper selection of their location may seriously hamper leak/burst detection and
125 localisation performance, the development of optimal sensor placement strategies is an
126 important area for research and validation. A case can be made that sensor placement, in
127 reality, is a multi-objective optimisation problem. There are many individual objectives, some
128 which are competing, which must be satisfied simultaneously. Therefore, selecting the
129 objectives which will be used to evaluate the quality of any given sensor configuration is a
130 critically important step in developing a sensor placement technique which reflects the reality
131 of the leak/burst localisation sensor placement problem. The definition of an ‘optimised’
132 sensor network depends on the context and design methodologies, relevant literature includes
133 effective contaminant detection (e.g. Ostfeld and Salomons 2004, Shastri and Diwekar 2006)
134 and model calibration - both hydraulic as in Kapelan et al. (2005) and water quality as in
135 Zhang et al. (2020). Sanz et al. (2016) proposed a leak-detection and localization approach
136 coupled with a (demand) calibration methodology that identifies geographically distributed
137 parameters. Tested on synthetic data they were able to correctly detect and locate leaks within
138 200m. Qi et al. (2018a) proposed a methodology to investigate the underlying capacity of
139 existing pressure sensors for pipe burst detection and thus provide practical guidance for
140 effective burst management (though not per se to provide optimised sensor placement) . Five
141 metrics were developed being: (1) undetectable nodes; (2) undetectable demands; (3)

142 detection dimensions (number of sensors that can simultaneously detect the bursts at each
143 node); (4) the spatial partition, where bursts within each partitioned region can be detected by
144 single sensor; and (5) the detectable threshold. All the metrics were calculated with the aid of
145 a pressure-driven hydraulic simulation model (including generating pipe burst scenarios), and
146 using Monte Carlo simulations to generate uncertain demand data. This work helps to
147 advance the understanding of pressure sensor deployment to burst detection. In Qi et al.
148 (2018b), similar work was presented for evaluating both hydraulic and water quality impacts.
149 Six proposed metrics focus on identifying different aspects of impacts as follows, (i) break
150 outflow volume, (ii) water shortage, (iii) nodes with significant pressure drops, (iv) pipes
151 with significantly decreased pressures, (v) pipes with reversed flow directions, and (vi) pipes
152 with significant increases in flow velocity. Computational simulation using hydraulic models
153 was used in a similar manner to the first paper for the case studies, based on calculating
154 metrics for each pipe break scenario. Two types of WDS case studies with varying attributes,
155 scales, and topologies were used to demonstrate the utility of the comprehensive framework,
156 although these did not include and field trials or real events for validation. Simulation results
157 showed that impacts of pipe breaks not only vary with pipe diameters but are also
158 significantly influenced by pipe locations, when the break occurs, and the specific metric
159 considered. The understanding and findings obtained offer important guidance to developing
160 effective pipe management / maintenance, resource planning and emergency response and
161 break restoration strategies.

162 Almost all the sensor placement algorithms for leak/burst localisation in a DMA rely on
163 modelling a large number of leak/burst scenarios. A number of hydraulic solver packages
164 exist which allow leaks/bursts to be modelled relatively easily, albeit often under the

165 (incorrect) assumption of a perfect (or at least well calibrated) model. Such a model needs to
166 closely match the physical and hydraulic conditions which exist in the real network.

167 Various methodologies (e.g. Casillas et al. 2015, Steffelbauer and Fuchs-Hanusch 2016,
168 Blesa et al. 2016) have been developed for selection of suitable sensor locations in order to
169 maximise sensitivity to leaks/bursts whilst minimising the required number of sensors (and
170 hence cost). Romano (2020) provides a detailed literature review of optimal sensor placement
171 in WDSs for leak/burst detection and localisation. The almost complete lack of field tests and
172 validation of the proposed techniques on real-life networks to assess their true value and
173 practicality was noted along with the fact that comparing the effectiveness of the different
174 proposed approaches remains an almost impossible task. Instead, tests and demonstrations of
175 proposed techniques nearly always involve synthetic numerical experiments. That said, a few
176 examples of field tests in the literature include the use of fire hydrants to simulate leaks.

177 Farley et al. (2013) performed validation with a total of eight hydrant openings conducted in
178 four DMAs. Six events were correctly localized to sub-DMA areas (ranging in size
179 approximately between 50% to 33% of the full DMA). Romano et al. (2020) successfully
180 approximately located a flushing event within a search area that was less than a quarter of the
181 total length of mains in the DMA. In Fuchs-Hanusch and Steffelbauer (2016) a comparison of
182 several methods including the methods proposed by Pérez et al. (2009), Casillas et al.
183 (2013b) and Steffelbauer and Fuchs-Hanusch (2016) was carried out by opening fire hydrants
184 to simulate different leak/burst scenarios in a real network and then assessing the leak/burst
185 localisation capabilities of the different methods by calculating the distance between the
186 suggested leak/burst locations and the opened fire hydrants. The results from the limited tests
187 carried out in that study showed that using different leak/burst positions and different sensor
188 sets, mainly those with sensors close to the leak/burst position, led to the best performance

189 (otherwise localisation was inaccurate as regards sub-areas). Huang et al. (2020) presented a
190 multistage bisection optimization approach to locate burst leaks within a DMA, where valve
191 operations and water balance analysis based on smart demand meters (required for all users in
192 the DMA, which is atypical) are iteratively performed to gradually narrow down the spatial
193 regions associated with leaks. They were able to transfer artificial burst leak analysis to
194 practical application for two leak regions (around 3-6% of the entire DMA) in a real WDS in
195 China.

196

197 **FRAMEWORK OF METHODS**

198 **Overview**

199 A novel, integrated framework of methods to achieve the dual aims of optimal sensor
200 placement and leak/burst localisation was developed which makes uses of a number of
201 interconnected techniques as depicted in Figure 1. The two key steps, in the order which they
202 are performed by the framework of methods are, to determine the optimal (or, more
203 generally, near optimal) configuration of pressure sensors by analysing a hydraulic model of
204 a DMA and subsequently, to analyse the pressure data from the optimal sensor configuration
205 to determine the approximate location of a new leak/burst which has been detected in a WDS.
206 Crucially the method utilises the same modelling results and geospatial search techniques in
207 both the placement and localisation.

208

209

210

211

212

213

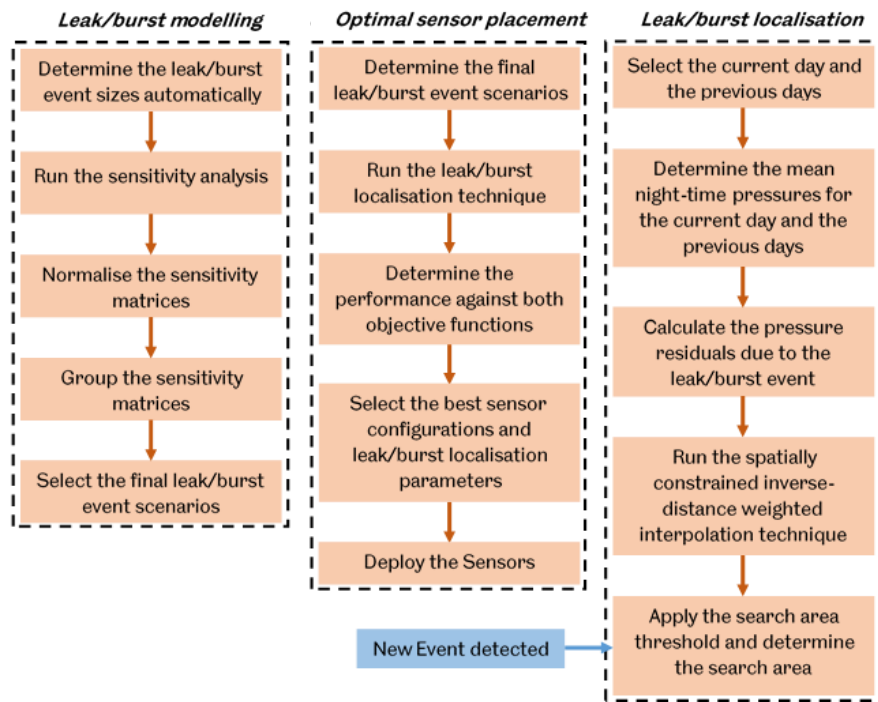
214

215

216

217

218



219

Figure 1: Schematic of the framework of methods

220

221 **Leak/ burst modelling**

222

The framework of methods requires a hydraulic model. This model does not require any special additional calibration, and the standalone models used in the case study were of a typical UK water company ‘top down’ calibration standard.

225

The first step is to model a range of leak/burst event sizes at various leak/burst event

226

locations throughout the DMA to build a sensitivity matrix. The sensitivity matrix contains

227

the changes in pressure for all potential sensor locations for all of the leak/burst event

228

scenarios (as in Farley et al. 2013). A mathematical representation of the sensitivity matrix is

229

shown in Equation 1.

230

$$S = \begin{bmatrix} \frac{p_1^{f_1} - p_1}{f_1} & \dots & \frac{p_1^{f_m} - p_1}{f_m} \\ \vdots & \ddots & \vdots \\ \frac{p_n^{f_1} - p_n}{f_1} & \dots & \frac{p_n^{f_m} - p_n}{f_m} \end{bmatrix} \quad (1)$$

232

233 Where $p_i^{f_j}$ is the pressure of sensor i when a leak/burst with constant flow, f_j , is present at
 234 node j , m is the number of node in the network (possible leak/burst locations – when leaks
 235 and burst are assumed as occurring at nodes), n is the number of sensors in the network and
 236 p_i represents the pressure of sensor i without the presence of a leak/burst in the network.

237 For each sensor configuration, the pressures corresponding to the selected sensor locations
 238 are extracted from the sensitivity matrix and analysed by the leak/burst localisation
 239 technique. For each leak/burst event the size of the search area (percentage of total pipe
 240 length) is determined and the average size of the search area is calculated for the sensor
 241 configuration, considering all leak/burst events. For any event which is not correctly localised
 242 the whole size of the DMA is counted to assign a poor level of localisation for that leak/burst
 243 event. The average size of the search area for all leak/burst events (including the penalty for
 244 incorrectly localising leak/burst events) is used to measure the quality of each sensor
 245 configuration.

246

247 **Optimal Sensor Placement**

248 A sensor placement technique minimises cost (numbers of sensors) whilst maximising
 249 performance when choosing where and how many sensors to place. The optimal sensor
 250 placement technique presented here is used to automatically determine the near optimal
 251 location of pressure sensors in a DMA to maximise the leak/burst localisation performance

252 whilst simultaneously using the minimum number of pressure sensors (which is a trade-off).
253 The sensor placement problem is formulated considering two objectives, namely the number
254 of sensors and level of localisation performance which can be achieved. These configurations
255 are specified with respect to multiple leak/burst event sizes which are determined
256 automatically for each DMA. The critical point of the optimal sensor placement technique is
257 that the leak/burst localisation technique is used by the optimal sensor placement technique to
258 determine the level of localisation performance for a given sensor configuration.

259 *Optimisation*

260 The GALAXY multi-objective evolutionary algorithm (MOEA) (Wang et al. 2017) is used to
261 search for the optimal sensor configurations in an efficient way due to the potential number
262 of possible configurations for DMAs of typical size. Once the maximum and minimum
263 number of sensors was set for a given DMA, the sensor placement technique only needed to
264 be run once to find all of the optimal configurations. The MOEA only requires two
265 parameters to be specified. These are the size of the population and the number of functions
266 evaluations (NFEs). The NFEs is the number of individual population members which are
267 evaluated using the objective functions and is equal to the population size multiplied by the
268 number of generations. This removes the main drawback of most GAs which need to specify
269 and fine-tune several parameters to ensure that the performance of the MOEA is acceptable
270 for the problem being considered. Following Wang et al. (2017), the amount of change
271 between successive generations was used to indicate convergence, and the number of
272 function evaluations was selected by running the sensor placement technique using several
273 DMAs to ensure that less than 0.1% performance improvement was attained in those cases
274 leading to a NFE of 100,000. A population size of 200 was chosen based on empirical tests
275 over multiple DMAs. The objective function used by the MOEA is formulated to minimise

276 the average size of the search area (percentage of DMA pipe length) and the number of
277 sensors at the same time so that the optimal solutions with different numbers of sensors can
278 be determined. The sensor placement technique determines the shape of the Pareto front (the
279 curve of trade-off between multiple objectives) to allow water company personnel to select
280 the appropriate number of sensors to deploy in a DMA.

281 The first objective function used by the optimal sensor placement technique evaluates the
282 ability of a sensor configuration to localise all possible leak/burst event scenarios which are
283 contained in the sensitivity matrix resulting from an event grouping technique. This
284 procedure was used to group together leak/burst event locations using only the changes in
285 pressure which were caused by them. An average localisation performance is determined
286 considering all of the event scenarios which are contained in the grouped sensitivity matrix.
287 The total weights of all graph links, which is the same as the length of the pipes that they
288 represent, in the search area is allocated as the size of the search area (percentage of DMA
289 pipe length). A penalty is applied to the size of the search area for an event which is not
290 correctly localised i.e. that the modelled leak/burst location is not one of the nodes in the
291 search area produced by the localisation technique. This penalty steers the population
292 generated by the MOEA towards sensor configurations which localise the greatest number of
293 events. A second penalty is also applied for any event for which multiple search areas are
294 produced by the localisation technique. A graph-based procedure, which uses the same graph
295 as the localisation technique was developed. If more than one search area is produced for an
296 event then, in the same way as for incorrect localisation, all of the graph links are counted as
297 being in the search area.

298 The second objective function used by the sensor placement technique is related to the cost of
299 each sensor configuration generated by the MOEA. The number of sensors which are being

300 installed is assumed by the sensor placement technique to be a proxy to cost. A sensitivity
301 analysis was conducted to investigate the best combination of leak/burst localisation
302 parameters (search area threshold and interpolation exponent) using two simple hydraulic
303 models.

304 *Hydraulic modelling*

305 The basis of many sensor placement techniques for leak/burst detection and localisation is
306 modelling a range of event scenarios so that the response of a DMA to these events can be
307 used to inform sensor locations. In this context the decision variables are the locations of the
308 sensors. A sensitivity analysis determines, for all possible combinations of leak/burst
309 locations and leak/burst event sizes, the changes to both the pressure and, in some cases flow,
310 which will occur. Due to practical considerations the optimal sensor placement technique
311 implemented considers fire hydrants as the set of potential sensor locations. For all sensor
312 placement runs in the case study a minimum value of three sensors and a maximum value of
313 ten sensors has been used.

314 Several parameters must be specified or determined prior to performing the sensitivity
315 analysis. The first two, which are related to the leak/burst events are the event sizes and the
316 event locations. Additionally, the allowable sensor locations must also be specified. Only
317 pressure data from these points can be considered. Next, a single run of the hydraulic model
318 is performed so that the normal pressures and flows are captured. These are used to determine
319 how much the pressure and flow has changed for each leak/burst scenario. The final step is to
320 iteratively add leak/burst events to the hydraulic model, one node at a time, and store the
321 changes in pressure which occur as a result.

322 A non-binarised sensitivity matrix is used as the input to the leak/burst localisation technique
323 used by the sensor placement technique. To normalise the sensitivity matrix, the changes in
324 pressure for each sensor location are divided by the normalisation factor, determined using a
325 hydraulic model specifically for each potential sensor location. This normalisation step and
326 the method for deriving the normalisation factors is used by both the sensor placement
327 technique and the leak/burst localisation technique to maintain consistency.

328 *Leak/burst event size*

329 An automated approach was developed to determine the minimum leak/burst event sizes to,
330 for each leak/burst event location, incrementally increase the leak/burst event size until one
331 potential sensor location registers a change in pressure which is greater than or equal to the
332 sensor accuracy. This ensures that only leak/event sizes which can be measured by at least
333 one sensor in the network being studied are considered for each leak/burst event size. It also
334 allows different leak/burst sizes or range of leak/burst event sizes to be determined for each
335 event location in a given network. A similar process is used to determine the maximum
336 leak/burst event sizes. However, the maximum event sizes are not calculated with respect to
337 the change in pressure but the increase in flow which occurs as a result of each event. To
338 achieve this, an additional parameter is used which is called the maximum allowable flow
339 increase. This parameter is a percentage which relates the average daily flow to the additional
340 flow which has occurred as a result of a modelled event considered by the sensor placement
341 technique, calculated during the analysis window.

342 Once the maximum and minimum leak/burst event sizes have been determined for all
343 leak/burst locations, and the validity of the event sizes are checked, the maximum and
344 minimum event size for the entire DMA can be determined which are used for the final event
345 size sensitivity matrices. For the purposes of the case studies presented a multiplier of 0.1 for

346 the maximum allowable flow increase, equivalent to 10% of the daily peak flow, was used as
347 this was felt to provide a good compromise biased towards finding smaller leaks (at risk of
348 running undetected) rather than larger (obvious surface water etc.) bursts. Once the leak/burst
349 event sizes have been determined a further novel step in the framework of methods is to
350 group together the leak/burst event scenarios according to the sensitivities. This optimisation-
351 based approach (similar to that first introduced by Sophocleous et al. 2019) reduces the
352 number of events which are considered by the sensor placement technique by grouping
353 together those event scenarios which are similar in terms of the sensitivities at all possible
354 sensor locations. The MOEA is also used for this step with the groups of event locations as
355 the decision variables. This process is repeated for all leak/burst events sizes, in turn.

356

357 **Leak/ Burst Localisation**

358 Pressure was utilised as the hydraulic variable to measure and analyse due to the much lower
359 cost and ease of installation of pressure sensors relative to flow sensors. Additional pressure
360 sensors, and the data collected from them, are central to the approach and it is crucial that the
361 (near) optimal combination of sensor locations are selected. This framework identifies the
362 minimum number of sensors, to minimise the associated cost of the sensors for a water
363 company, whilst simultaneously maximising the performance of the deployed sensor
364 configurations.

365 The sensor placement and leak/burst localisation techniques both rely upon the fact that the
366 characteristics of a new leak/burst event will lead to a specific set of effects on the hydraulics
367 of the DMA which can be measured and used to infer the approximate location of the
368 leak/burst event (by solving the inverse problem). There will be differences between the

369 effects depending upon whether the event is modelled or is in a real WDS because a
370 hydraulic model cannot perfectly match the real WDS, in addition monitoring data is never
371 completely accurate. Once the optimal configuration of pressure sensors has been determined
372 for the technique within certain limits using leak/burst simulations in a hydraulic model, and
373 the pressure sensors have been deployed then the novel leak/burst localisation technique can
374 be run when a new leak/burst is detected.

375 The framework of methods is designed and targeted towards leaks/bursts not reported by
376 customers, i.e. leaks that do not result in surface water or other obvious effects. These events
377 can easily be masked by the higher flows which are typically seen during the day but this
378 problem is improved by assessment during the night-time period. To achieve this the
379 leak/burst localisation technique can estimate the area (by providing a set of DMA pipes)
380 containing the new leak/burst event by comparing the night-time pressure signals after the
381 leak/burst event has occurred with recent signals, not modelling results so reducing the
382 dependency on model accuracy. The magnitude of the change in pressure, measured by each
383 deployed pressure sensor, is then used as the basis for leak/burst localisation. This means that
384 there can be, at least, 24 hours between the commencement of the leak/burst event and the
385 approximate location being calculated. Using the night-time pressure maximises the
386 detectability of the change in pressure effects of the leak as there are minimal other demand
387 induced variations.

388 A novel spatially constrained version of the inverse distance weighted (IDW) - referred to
389 hereafter as SC-IDW - interpolation technique (Zimmerman et al. 1999) is used here to
390 determine the location of new leaks/bursts occurring in a DMA. In IDW interpolation, the
391 estimated value at unmeasured locations is determined as a weighted sum of the measured

392 values where the weight for each measured location is based upon its proximity to the
393 location being estimated. It can be mathematically described as in Equation 2.

394

$$395 \quad Z_{est,j} = \sum \frac{z_i}{[d_{ij} + s]^p} / \sum \frac{z_i}{[1 + s]^p} \quad (2)$$

396

397 where; $Z_{est,j}$ = estimated value at location j, z_i = measured sample value at location i, d_{ij} =
398 distance between i and j, s = smoothing factor (set to 0), p = weighting power or exponent
399 (range = 1-6).

400 The leak/burst localisation technique analyses of the data collected from the additional
401 pressure sensors in a DMA over a number of days to determine the change in pressure
402 (expressed as residuals) at each sensor location due to the new leak/burst. The novel, SC-
403 IDW interpolation (Boatwright et al. 2016) then estimates the changes in pressure at all
404 locations throughout the DMA to identify the area with the highest change in pressure, which
405 is considered as the most likely area in the DMA containing the new leak/burst event. The
406 distances used by the novel SC-IDW interpolation technique are determined as the shortest
407 distance travelled between two points in the DMA (rather than using Euclidean distance). The
408 distances are determined from an undirected graph which is automatically derived from a
409 hydraulic model (as a two-dimensional square matrix of nodal distances).

410 One of the advantages of using SC-IDW interpolation, as opposed to more complex spatial
411 analysis techniques, is that only a single parameter needs to be specified. This is the exponent
412 used to calculate the weights between nodes, which depend upon the distance between them.
413 The effect of the exponent is to control the amount of influence that near measured locations
414 have when compared to distant measured locations on the value at the unmeasured point
415 which is being estimated. The exponent influences the shape of the surface which is produced
416 and using higher values of exponent tends to have a smoothing effect on the interpolation

417 surface. Different values for the interpolation exponent have been used depending upon the
418 domain and application (de Mesnard 2013). A process for automatically determining the best
419 value of the interpolation exponent was developed to overcome this. Once the SC-IDW
420 interpolation technique has been performed, the next step is to determine which parts of the
421 DMA should be searched. The area with the largest estimated change in pressure is most
422 likely to be in proximity to the leak/burst event so a method of dividing the surface of
423 estimated values of the change in pressure is required. The search area threshold,
424 ***threshold_{sa}***, is used to perform this which is set as a proportion of the range of values on
425 the interpolation surface determined for a leak/burst event and can take any value between 0
426 and 1. Any locations on the interpolation surface with an estimated value which is above the
427 numerical threshold (see equation 3) is designated as part of the search area.

$$428 \quad x_{sa} = z_{j,min} + \mathbf{threshold}_{sa}(z_{j,max} - z_{j,min}) \quad (3)$$

429 Where x_{sa} is the numerical value of the threshold, z_j are the estimated changes in pressure
430 for all locations for a single leak/burst event.

431 This information is then passed on to field teams to direct the search for the leak/burst event.
432 The value of the search area threshold affects the proportion of the DMA which is included in
433 the search area. The amount of the DMA which is in the search area is a measure of the
434 localisation performance for a leak/burst event. The sensor placement technique
435 automatically determines the best value for the search area threshold whilst determining the
436 optimal sensor configurations.

437

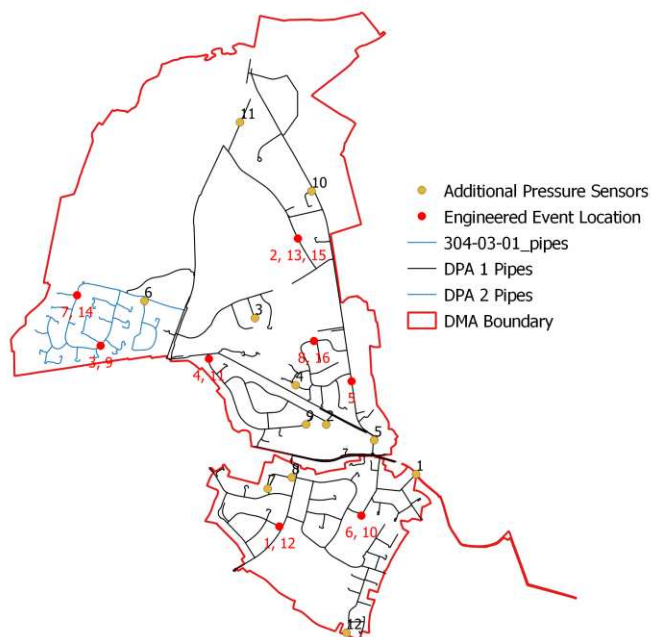
438

439 **CASE STUDY**

440 **Overview**

441 A case study involving a DMA which had not been used in the development and verification
442 of the framework of methods was used for validation. The combined performance of the
443 sensor placement technique and the leak/burst localisation technique was determined by
444 applying them both to the same DMA using data from engineered events (by flushing from
445 hydrants) and industry standard hydraulic models.

446 The validation DMA, situated in a small urban town, is connected to a single service
447 reservoir which has a standard diurnal profile. 12 additional sensors were deployed (non-
448 optimally and for a variety of purposes) in the DMA as illustrated in Figure 2 (in which the
449 locations of the engineered events are shown as red circles). The DMA is split into two
450 discrete pressure areas (DPAs). The pressure in one of these is controlled using a pressure
451 reducing valve (PRV) to regulate the pressure at a sufficient level as to maintain the
452 minimum required pressure whilst also ensuring that there is not excessive pressure. All of
453 the pressure sensors collected a pressure measurement every minute for a period of four
454 months. The sensors were manually spread evenly throughout the validation DMA by water
455 company staff to ensure that the entire DMA was covered in spatial terms (using the
456 hydraulic model and GIS). These 12 hydrant locations (rather than all fire hydrants)
457 effectively formed a constrained version of the sensor placement technique that was used to
458 validate the framework.



459

460 **Figure 2:** The 12 deployed sensor locations and DPAs for the validation DMA

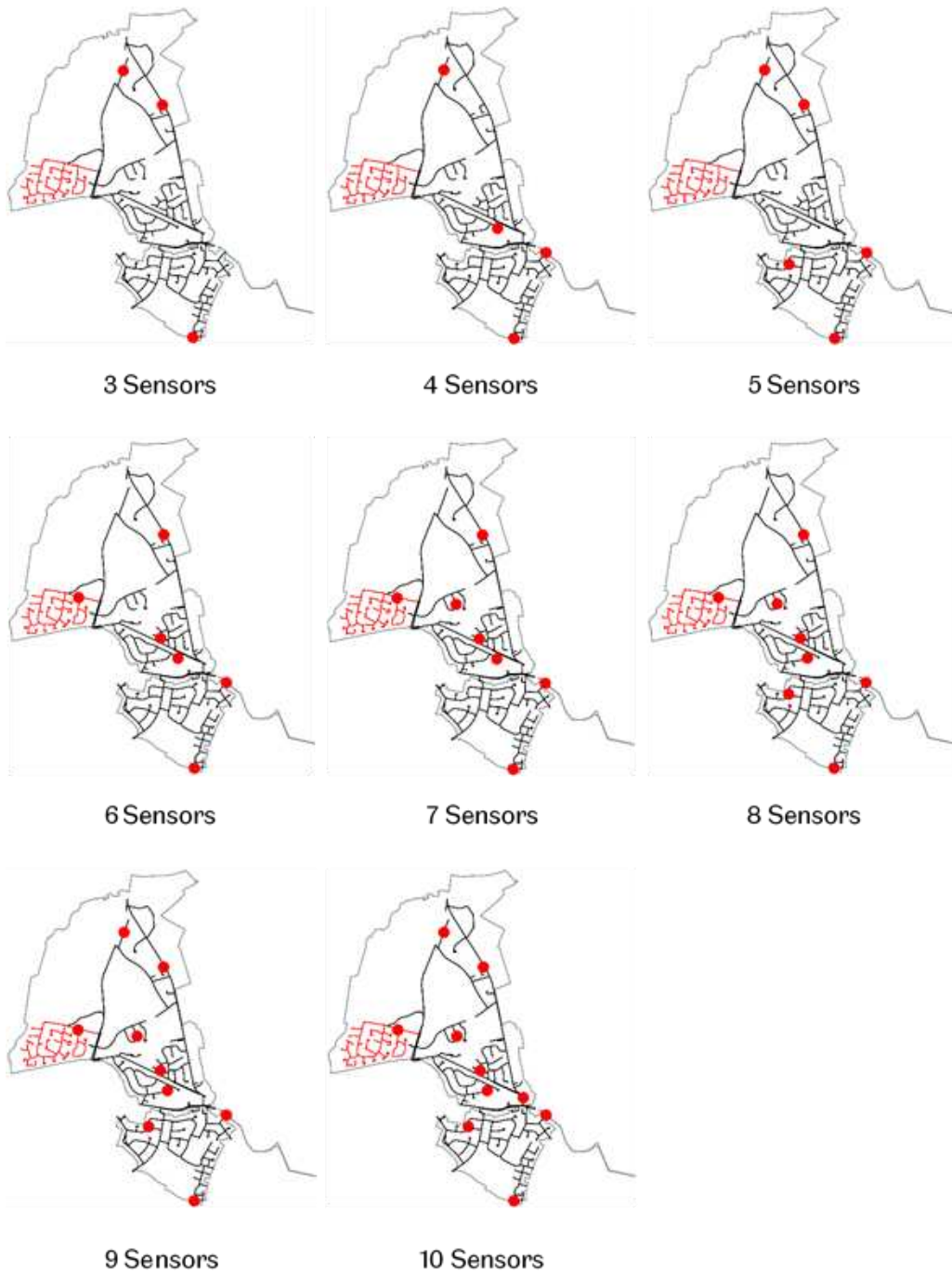
461 **Sensor placement**

462 Optimal sensor configurations with between 3 and 10 sensors (inclusive) were determined. In
 463 addition to identifying the optimal sensor configurations, some baseline sensor configurations
 464 were selected at random from the available sensor locations in the validation DMA, these
 465 were based on expert human judgement (academic modeller). Baseline configurations with
 466 between 3 and 10 sensors (inclusive) were selected so that a comparison of the performance
 467 of the baseline and optimal sensor configurations could be completed for all numbers of
 468 sensors considered. The baseline level of performance was used to represent the typical level
 469 of leak/burst localisation performance which would be achieved if sensors were deployed at
 470 random without using the sensor placement technique.

471 The optimal sensor configurations, which were constrained by the deployed sensor locations,
472 were determined. Figure 3 shows these for the optimal case. Once the optimal sensor
473 configurations were determined for the DMA, and combinations of parameters were found,
474 the leak/burst localisation performance was determined for each engineered event that is; the
475 size of the search area (percentage of DMA pipe length), whether the event was correctly
476 localised and whether multiple search areas were determined. The average size of the search
477 area, across all engineered events, was used as the measure of performance for each of the
478 optimal sensor configurations. The same penalties for producing multiple search areas and
479 incorrectly localising leak/burst events used by the sensor placement objective function were
480 applied to the engineered events. This allowed a direct comparison to be made between the
481 leak/burst localisation performance achieved using modelled data and real data collected
482 during engineered events.

483

484



485 **Figure 3:** Optimal sensor configurations (red circles) with varying numbers of sensors for the
 486 validation DMA

487 To determine the maximum and minimum leak/burst event sizes an event size increment of
 488 $0.11/s/m^{0.5}$ was specified. The maximum allowable increase in flow was specified as 0.1
 489 which equated to a 10% increase in the flow relative to the maximum daily flow. The
 490 automatically determined leak/burst event sizes and the corresponding results from the

491 leak/burst event grouping technique are provided in Table 1. For each of the considered
492 leak/burst event sizes, in the first column, the number of valid leak/burst event groups
493 produced are given in the second column.

494 **Table 1:**

495 **Engineered Events**

496 In a similar fashion to the deployed sensor locations, the engineered event locations were
497 manually chosen to ensure that at least one engineered event was conducted in each section
498 of the DMA. The sizes of the engineered events were selected to be just sufficiently large to
499 be distinguishable from anomalous but legitimate customer demand which could still occur,
500 even during the night.

501 The locations of the engineered events for the validation are shown as red circles in Figure 2.
502 The indices for each event location are given by the red numbers next to the locations. Some
503 event locations were used multiple times, providing replication, on different days such that 8
504 unique hydrants were opened across the 16 engineered events.

505 The engineered events were conducted during the period of minimum flow which is used by
506 the leak/burst localisation technique. Each event was started before 03:00am and ended after
507 04:00am. The opening of each hydrant was controlled to achieve an approximate flow rate of
508 0.6 l/s at the start of the event and the same hydrant opening was maintained for the duration
509 of the engineered events.

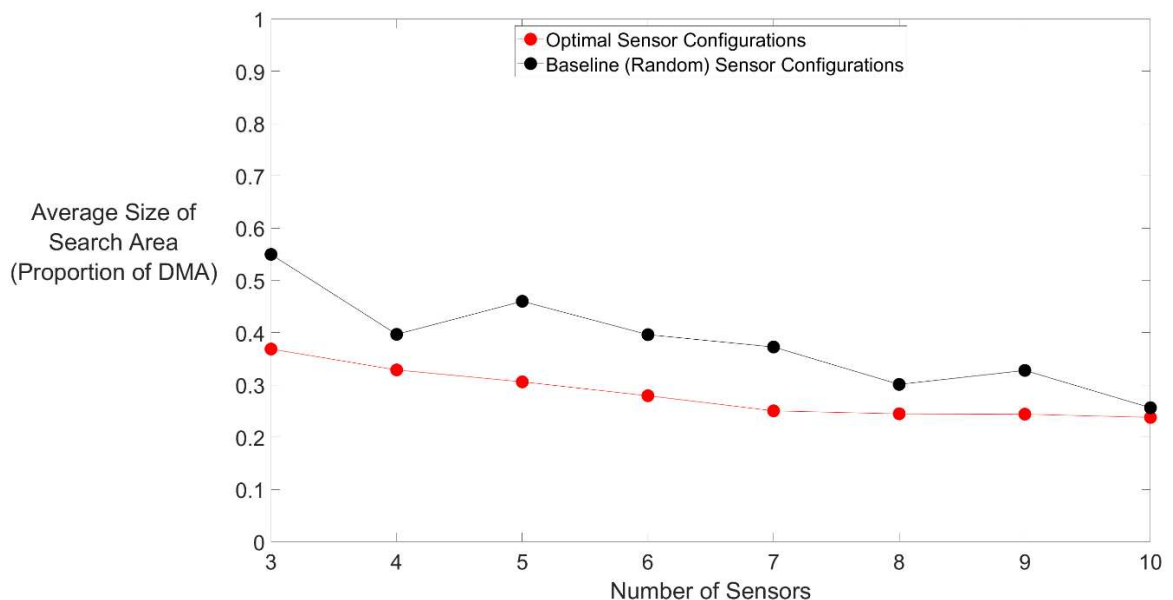
510

511

512 **COMPUTATIONAL RESULTS**

513 **Pareto front for optimal versus baseline performance**

514 The Pareto front for the constrained optimal sensor configurations and parameters and the
515 performance achieved for the baseline sensor configurations and parameters are shown in
516 Figure 4. For all numbers of sensors, the constrained optimal sensor configurations
517 outperformed the baseline sensor configurations, as expected. The difference in performance
518 between the optimal and baseline configurations and parameters ranged from 18.1%, for the
519 cases with 3 sensors, and 1.9% for the case with 10 sensors.



520 **Figure 4:** Comparison of the performance for the constrained optimal and baseline sensor
521 configurations for validation DMA

522 **Overall results**

523 The performance of the leak/burst localisation technique, when applied to the each of the
524 engineered events in the DMA, is given in Table 2. For each engineered event, the size of the
525 search area (percentage of DMA pipe length) and whether the event was correctly localised
526 within this are shown for each optimal sensor configuration. Correctly localised events are

527 denoted by bold text and an asterisk denotes events for which multiple search areas were
528 produced. At the bottom of the table the equivalent value for the objective function,
529 accounting for both objective function penalties, is given so that results obtained using the
530 modelled data and the real data can be compared.

531

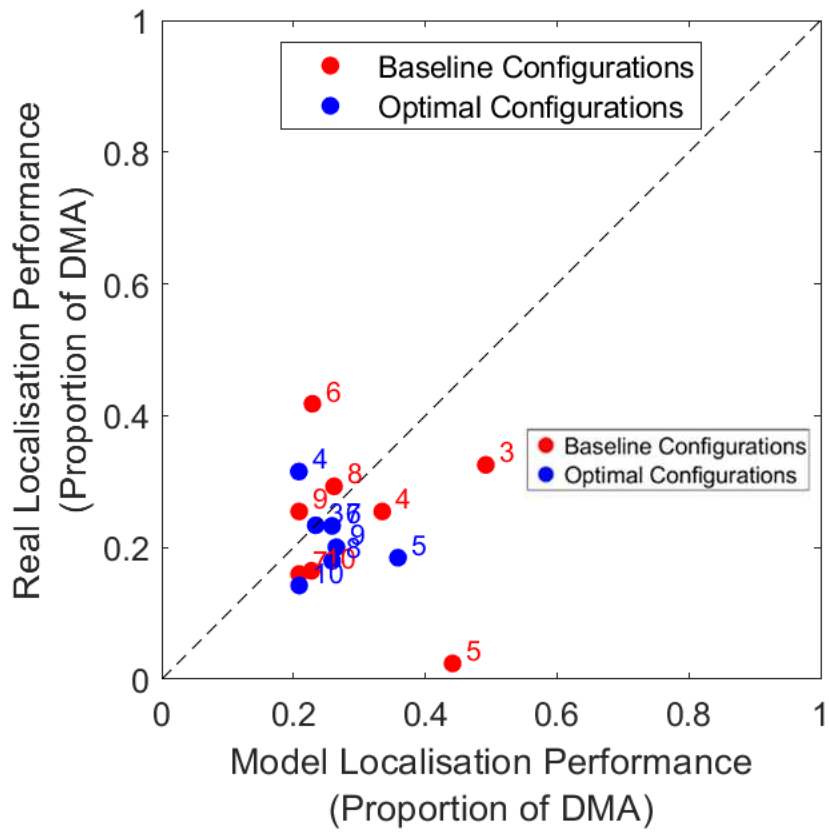
532 **Table 2**

533 **Engineered versus modelled results**

534 A comparison between the localisation performance was conducted for engineered event 8. In
535 Figure 5, the size of the search area produced using the modelled data has been plotted on the
536 x-axis and the size of the search area determined using the engineered event data was plotted
537 on the y-axis. A dashed black line, representing the line of perfect agreement between the
538 modelled and real engineered event performance is also shown. The proximity of each of the
539 optimal and baseline sensor configurations to the black line denotes the level of agreement
540 between the two. In the ideal case, the size and location of the search area would be identical
541 for both the modelled and the real engineered event when the same number of sensors are
542 considered. Of all the sensor configurations only the optimal sensor configuration with 3
543 sensors showed perfect agreement between the search areas determined using the hydraulic
544 model and the engineered event. The agreement for this sensor configuration was perfect
545 even though there was a difference between the relative changes in pressure determined using
546 the hydraulic model and for the engineered event. The level of agreement, denoted by the
547 proximity of each configuration to the line of perfect agreement, for the optimal sensor
548 configurations was higher than for the baseline sensor configurations. Other optimal
549 configurations demonstrate how the leak/burst localisation technique can be used with some

550 level of reasonable accuracy even when a very well calibrated hydraulic model is not
551 available for use by the sensor placement technique.

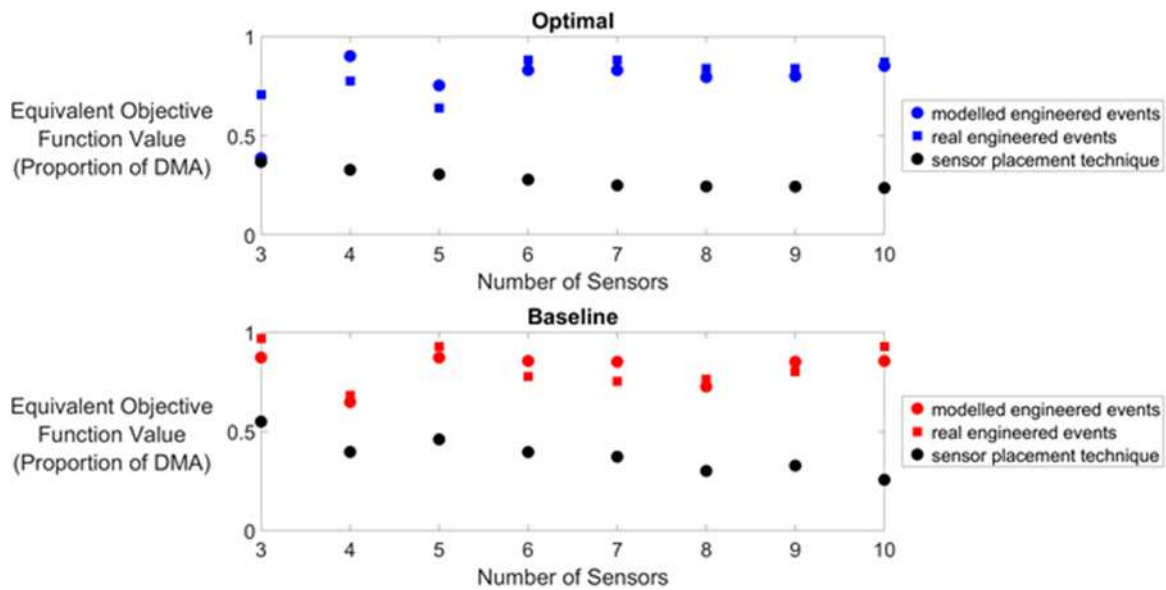
552



553 **Figure 5:** Agreement between the modelled and real search area sizes (percentage of DMA
554 pipe length) for engineered event 8 using the optimal and baseline sensor

555 **Baseline versus constrained results**

556 One key factor which influenced the leak/burst localisation results in Table 2 for the optimal
557 (and baseline) sensor configurations was that the optimal and baseline sensor configurations
558 were determined using a range of leak/burst event scenarios. It is informative in assessing the
559 performance of the technique to determine what the expected level of leak/burst localisation
560 performance was for the size (flow rate) of the engineered events, in the same way as for the
561 sensor placement technique, so that they could be more directly compared. The search areas
562 (percentage of DMA pipe length) determined by the leak/burst localisation technique using
563 the modelled data for each of the engineered events, were corrected to account for the two
564 penalties applied within the sensor placement objective function. The same correction was
565 also applied to the search areas determined using the real engineered event data. The Pareto
566 front obtained by running the constrained sensor placement technique was plotted against the
567 corrected average search areas for the constrained optimal and baseline sensor configurations
568 as shown in Figure 6. The constrained optimal configuration was selected from only 12
569 locations whereas the results plotted in black were determined using the sensor placement
570 technique selecting from 145 hydrants. The Pareto fronts, determined by the sensor
571 placement technique considering all of the leak/burst event scenarios determined by the event
572 grouping procedure, are plotted in black.



573 **Figure 6:** Comparison of the equivalent objective function values for the baseline and
 574 constrained optimal sensor configurations

575 A clear trend is that the leak/burst localisation performance achieved for the constrained
 576 optimal sensor configurations agrees very well when the modelled engineered events are
 577 compared to the real engineered events. Aside from the configuration with 3 sensors, the
 578 remaining constrained optimal configurations produced average search areas within 10% of
 579 each other. As the number of sensors increases the agreement between the results also
 580 improves, demonstrating that comparable performance was achieved even when a water
 581 industry standard hydraulic model was used to model the engineered events. By comparing
 582 the sensor placement results, plotted in black, with the modelled engineered events it was
 583 clear that the selected engineered event locations and sizes were much more difficult to
 584 localise. The only possible reason for this, aside from the different leak/burst event sizes and
 585 locations, was that the results plotted in blue were determined using the constrained optimal
 586 configuration.

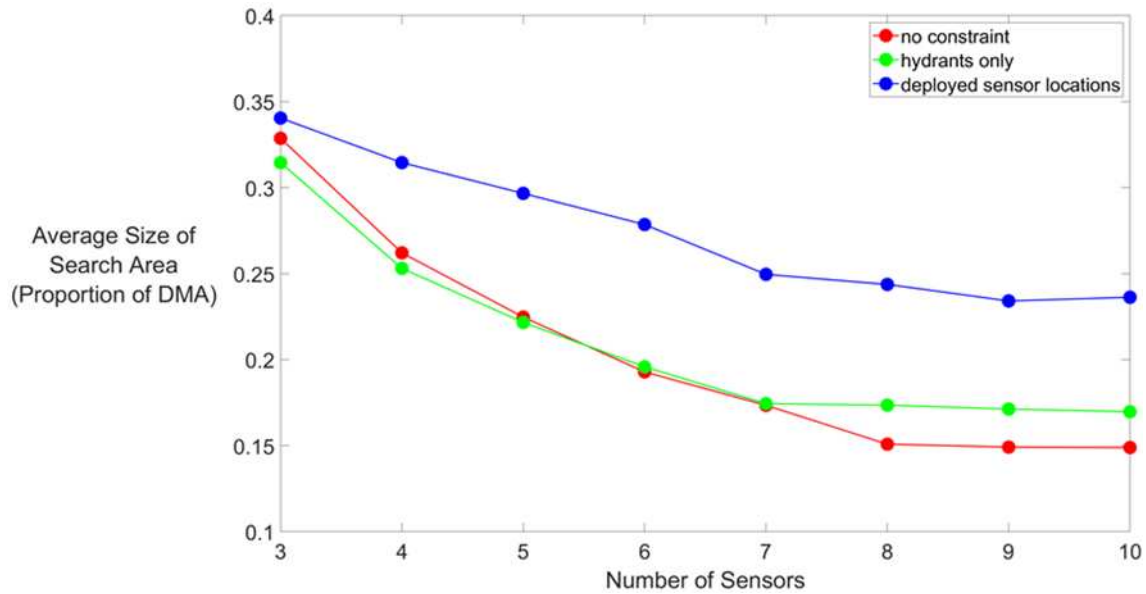
587

588 Limiting the sensor placement technique to consider only the 12 deployed sensor locations
589 resulted in there being a high degree of similarity between the constrained optimal and
590 baseline sensor configurations. The fact that the performance achieved using the modelled
591 engineered events for the baseline sensor configurations agreed more closely to the sensor
592 placement technique than for the constrained optimal configurations indicates that the
593 baseline configurations were more favourable for localising the set of engineered events.
594 Constraint on the available sensor locations combined with extremely small engineered
595 events made localisation difficult and essentially meant that the random and baseline
596 performed very similarly. The agreement between the engineered events and their modelled
597 equivalents was used as justification that the sensor placement objective function could
598 accurately predict leak/burst localisation performance (the agreement was good for both
599 baseline and optimal).

600 **Pareto fronts for constrained sensor placement technique**

601 The constraint included in the sensor placement technique, which limited the available sensor
602 locations to only hydrants, has a limiting effect on the sensor configurations which can be
603 made and on the resulting sensor placement performance. This is also true for the constraint
604 due to the deployed sensor locations for validation. Therefore, a comparison between the
605 Pareto fronts for several different versions of the sensor placement technique, with varying
606 levels of constraint on the sensor locations, was conducted to determine the effect on
607 performance of the sensor placement technique. In Figure 7 the sensor placement
608 performance, measured using the average size of the search areas produced (over the
609 engineered events), is plotted against the number of sensors for the three different levels of
610 constraint.

611

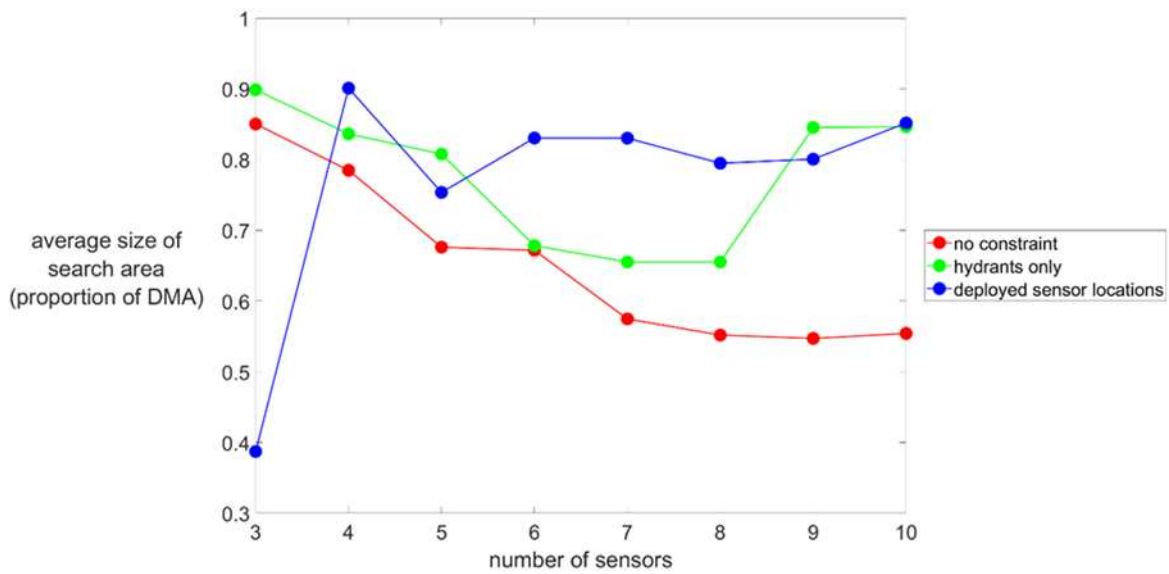


612 **Figure 7:** Comparison of the sensor placement performance for three levels of constraint of
 613 the sensor placement technique

614 The most constrained version, plotted in blue, is limited to just 12 deployed sensor locations
 615 (see Figure 2) and the least constrained version, plotted in red, could choose from 731
 616 junctions in the hydraulic model. Between these two, plotted in green, the sensor placement
 617 technique could choose from 145 hydrants in the DMA. The lower the level of constraint,
 618 were there were more potential sensor locations to choose from, the better the sensor
 619 placement technique performed. The most constrained version of the sensor placement
 620 technique which only considered the 12 deployed sensor locations (blue) performed worse.
 621 The version with no constraint (red) performed very similarly to the version considering
 622 hydrants (green) for the cases with fewer than 8 sensors but when 8 or more sensors were
 623 considered the version with no constraint performed better by between 2-3% of the DMA.
 624 Hence, constraining to hydrants was only a little different to allowing any node as potential
 625 sensor location thus minimising the reduction in the leak/burst localisation performance.

626 The average size of the search areas produced, including the penalties for incorrect
 627 localisation and multiple search areas, for all 16 engineered events was determined for each

628 number of sensors. The results for the three level of constraint are plotted in Figure 8 as
 629 regards leak/ burst localisation performance.



630 **Figure 8:** Comparison of the leak/burst localisation performance for the 16 modelled
 631 engineered events for three different levels of constraint of the sensor placement technique

632

633 The least constrained version of the sensor placement technique, where all hydraulic model
 634 junctions were considered as valid sensor locations, performed best overall. The sensor
 635 configurations used in this figure were determined with respect to all events used by the
 636 sensor placement technique and not the 16 modelled events. Aside from the case with three
 637 sensors, smaller average search areas were produced for all sensor configurations than for
 638 either of the two other constraint levels. As the constraint was increased, by considering all
 639 hydrants as valid sensor locations, a marked decrease in the leak/burst localisation
 640 performance was seen. The most constrained version of the sensor placement technique,
 641 which considers only the 12 deployed sensor locations, was, on average the worst
 642 performing. By comparing the results in Figure 7 with those in Figure 8 the effect of only
 643 considering a small number of leak/burst events was clear. The localisation results in Figure 8

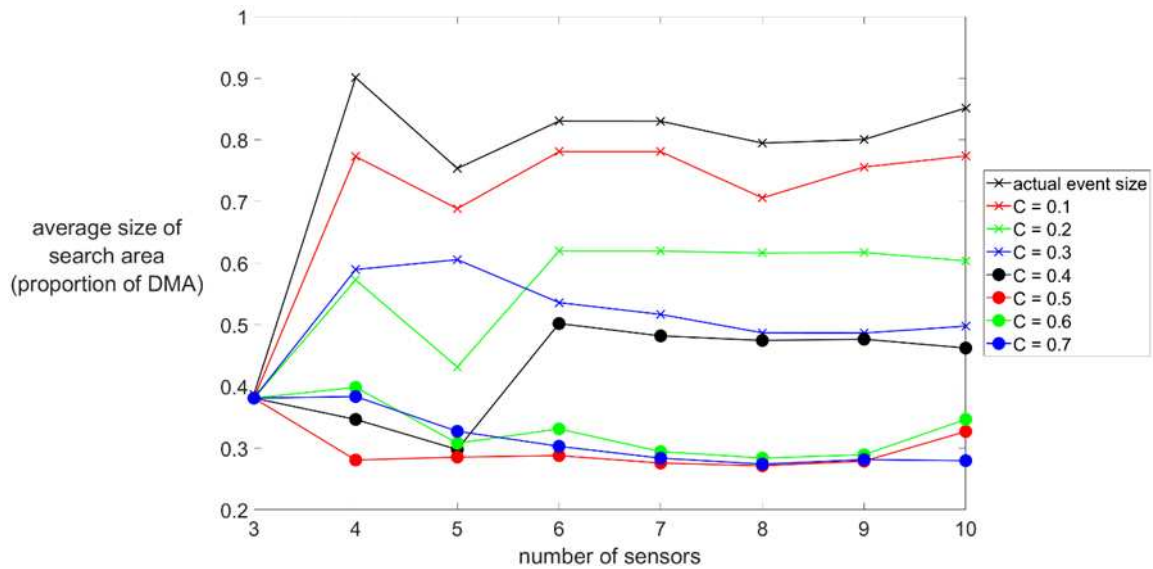
644 did not produce smooth lines since the smaller number of event locations considered was
645 much more sensitive to individual sensor locations. By comparing the green and blue lines in
646 Figure 8 the effect of constraining the sensor placement technique to only selecting from the
647 deployed sensor locations illustrated that the effect was to reduce the leak/burst localisation
648 performance by approximately 1%. For the sensor configurations with more than 3 sensors
649 the average reduction in localisation performance was approximately 6% of the size of the
650 DMA. Concerning the case with 3 sensors for the deployed sensor locations (blue line)
651 unexpectedly good performance was seen compared to other sensor configurations and levels
652 of constraint. This was because the sensor configurations were determined relative to all
653 possible leak/burst locations but the results shown pertain to only the engineered event
654 locations. In this case, using 3 sensors enabled the leak/burst localisation technique to
655 correctly localise more events than configurations with more sensors, reducing the applied
656 penalty and thereby improving the average performance.

657

658 **Effect of small engineered event sizes**

659 Figure 9 demonstrates that the small size of the engineered events negatively impacted the
660 leak/burst localisation performance when compared to the range of event sizes generated by
661 the sensor placement technique. As the leak/burst event size increased the average size of the
662 search area decreased across the 16 modelled engineered events. The emitter coefficient of
663 0.5 produced the smallest average search areas and further increases in event size above this
664 did not lead to further reductions in the average search area size. The actual size of the
665 engineered events led to the significantly worse performance than for any of the event sizes
666 determined by the sensor placement technique. Comparing the actual event sizes (black line
667 with crosses) with the worst performing of the determined leak/burst event sizes ($C = 0.1$ -

668 red line with crosses) the average reduction in performance was on average approximately
 669 6% of the DMA. For the best performing of the determined leak/burst event size ($C = 0.7$ –
 670 blue line with circles) the reduction in performance was 47% of the DMA on average.
 671 Therefore the small size of the leak/burst events was more impactful than using the
 672 constrained version of the sensor placement technique.



673 **Figure 9:** Comparison of the leak/burst localisation performance for 16 modelled events
 674 considering different sizes of event using the constrained optimal sensor configurations

675

676 **DISCUSSION**

677 The framework developed is integrated so that the leak/burst localisation technique is used by
 678 the sensor placement technique to determine the optimal configuration(s) of pressure sensors.
 679 The only difference is that real data is used by the leak/burst localisation technique whereas
 680 hydraulic model simulated data is used by the sensor placement technique. This ensures that
 681 the sensor configurations consider not only the hydraulic changes which are caused by
 682 leak/burst events but also the technique which is being used to localise them. A range of

683 optimal sensor configurations are determined, although this is not guaranteed for every DMA,
684 so that they can be presented to decision makers in the form of a Pareto front to make an
685 informed decision considering the trade-off between the number of sensors and the leak/burst
686 localisation accuracy. Field teams can use this information to focus the search for the
687 leak/burst event so that it can be precisely located and repaired. This framework presented
688 can be easily adapted for any data-driven or model-based leak/burst localisation technique
689 including the traditional approaches which are currently mainly used by many water utilities
690 such that the localisation accuracy, including the number of leak/burst events correctly
691 localised, is maximised.

692 The leak/burst localisation technique is data-driven and does not require a calibrated
693 hydraulic model. Many leak/burst localisation techniques are developed for use with
694 hydraulic model data only, in other words they only ever use simulated data and this poses
695 serious transferability problems to real WDSs (e.g. Marzola et al. 2022). Model-based
696 leak/burst localisation techniques are highly sensitive to the quality of model being used and
697 will only perform well when a highly calibrated model is available. The sensor placement
698 technique does not rely on a very well-calibrated hydraulic model, instead a UK industry
699 standard calibrated model, because the leak/burst localisation technique uses the differential
700 changes in pressure throughout the DMA to infer the approximate location of a leak/burst
701 event.

702 Evaluating performance using engineered events gives greater confidence in the achieved
703 results than solely using model simulations when related to the achievable performance on
704 real leak/burst events in WDSs. The past pressures are determined for each pressure sensor in
705 the DMA, calculated over 14 nights, and then compared to the pressure in the presence of a
706 new leak/burst event. Using the night time means that the uncertainty in the customer

707 demands is minimised and this has less influence over the leak/burst localisation
708 performance. This is also aided by the use of the SC-IDW technique because, for every
709 location in a DMA, multiple pressure sensors are used to estimate the change in pressure.
710 This reduces the reliance on a single sensor which, in turn, reduces the influence of sensor
711 uncertainty on the determined search area. The SC-IDW technique is an improved version of
712 IDW interpolation which accounts for the layout of pipes in a DMA. By using the novel
713 distance function (calculated using the shortest path along pipe lengths) as opposed to
714 Euclidean distance, more realistic and often smaller search areas were produced than when
715 compared to Romano et al. (2013). The novel distance function is able to distinguish between
716 two pipes which are close together but which are not connected directly to each other which
717 represents a significant improvement over results from Romano et al. (2013) where pipes
718 which are distant, in terms of the length travelled along pipes, were still included in the area
719 with the highest probability of a leak/burst event.

720 Leak/burst events as small as 3.5% of the peak daily flow were correctly localised using as
721 few as 3 optimal pressure sensors. This compares favourably with the technique developed by
722 Soldevila et al. (2019) which localised (to within 200m) a leak/burst event at night of
723 approximately 8% of the peak inflow using 5 sensors. This performance was achieved even
724 though the size of the engineered events was smaller than the minimum theoretical leak/burst
725 event sizes determined prior to running the sensor placement technique.

726 This is the first automatic procedure for determining a range of leak/burst event sizes for
727 sensor placement in a DMA for the purpose of leak/burst localisation. A previous attempt at
728 reducing the size of the search space by Sophocleous et al. (2019) grouped together the
729 leak/burst events by proximity. However, even leak/burst events which are close together can
730 have very different effects on a DMA. Using the effect on pressure directly to group the

731 leak/burst events overcomes this problem. A further novel procedure, developed as part of the
732 sensor placement technique, groups together the leak/burst event scenarios to reduce the
733 number of leak/burst events which must be considered by sensor placement.

734 The number of additional pressure sensors deployed throughout a DMA is a critical factor
735 which dictates the achievable leak/burst localisation performance. The improvement in both
736 localisation and sensor placement performance diminished as higher numbers of sensors were
737 considered meaning that water utilities would likely prefer to deploy fewer sensors although
738 this would depend upon their strategic aims.

739 The potential sensor locations were limited to hydrants only. Despite this, leak/burst
740 localisation performance reduction was found to be only around 2-3% when compared to
741 considering all junctions as candidate sensor locations. As illustrated in Figures 7 and 8, the
742 constraint of only selecting from the hydrant locations did not lead to a significant reduction
743 in sensor placement performance, indicating the validity for such a constraint particularly in
744 light of the ease of installation and the reduced cost of deploying sensors at hydrants.

745

746 **Further Work**

747 A number of avenues are apparent for development of this system in future work. Firstly, a
748 study could be conducted to determine the relationship between the level of hydraulic model
749 calibration and the sensor configurations which are determined as a result. Further to this the
750 leak/burst localisation performance, determined using engineered events, can be ascertained
751 for the optimal sensor configurations with varying levels of hydraulic model calibration.

752 A detailed cost-benefit analysis could be performed for deploying additional pressure sensors
753 for leak/burst localisation and built into the sensor placement technique. There is a cost which

754 can be associated with each type of individual leak/burst event which can occur in a DMA
755 which is related to regulatory targets (and associated penalties) and the cost of repairing it.
756 For each DMA, an associated cost of leak/burst events can be determined and compared to
757 the cost of deploying pressure sensors.

758

759 **CONCLUSIONS**

760 A framework of methods has been developed to localise new leak/burst events in WDS using
761 a data-driven leak/burst localisation technique integrated with a sensor placement algorithm
762 and utilising the same modelling results and geospatial search techniques in both. The
763 leak/burst localisation technique is used by the sensor placement technique ensuring that the
764 determined sensor configurations are optimal with respect to the leak/burst localisation
765 technique. The localisation technique does not require a hydraulic model to be compared with
766 the measured pressures from a real DMA which reduces its reliance on a highly calibrated
767 hydraulic model when compared to model-based leak/burst localisation techniques. Multiple
768 leak/burst event sizes and locations were considered in real world engineered events ensuring
769 that the range of leak/burst event scenarios of interest, namely those events which are
770 typically unreported and cause changes in pressure throughout a DMA, are used to determine
771 the optimal sensor configurations. Key findings include:

- 772 • The sensor placement technique was used to determine a Pareto front of optimal
773 sensor configurations (and parameter combinations) with varying numbers of sensors.
774 A MOEA was used to determine the sensor configurations and combinations of
775 parameters which simultaneously minimises the required number of sensors and
776 maximises the localisation performance.

- 777 • The distance used by the SC-IDW interpolation technique is determined as the
778 shortest path between two points in a DMA travelling along the pipes ensuring the
779 topology of the pipes in the DMA is respected unlike using Euclidean distance as per
780 traditional IDW interpolation.
- 781 • By incorporating the novel sensor placement technique into the integrated framework
782 (and using the same SC-IDW interpolation technique) the leak/burst localisation
783 accuracy can be improved. This was demonstrated by comparing the localisation
784 performance of the integrated framework against a baseline sensor placement
785 technique.
- 786 • A novel procedure for determining the smallest and largest leak/burst event size for all
787 considered leak/burst event locations was developed. This automatic procedure
788 requires the specification of three parameters so that all leak/burst event sizes can be
789 determined for an entire DMA.
- 790 • A novel leak/burst event grouping procedure was used to group together leak/burst
791 event locations using only the changes in pressure which were caused by them. This
792 significantly reduced computational effort and ensured that leak/burst events which
793 caused very similar changes in pressure for all candidate sensor locations were not
794 considered separately by the sensor placement technique.
- 795 • A total of 16 engineered leak/burst events, by opening fire hydrants, were carried out
796 in a real DMA to conduct framework validation. The constrained optimal sensor
797 configurations were determined from the deployed sensor locations by using a heavily
798 constrained version of the sensor placement technique. Constraining to hydrants was
799 almost the same as allowing any node as potential sensor location, and which results
800 in a no-dig solutions in practice. Baseline sensor configurations were also selected at

801 random from the deployed sensor locations and a comparison between the optimal
802 and baseline configurations was conducted.

- 803 • Validation demonstrated that the novel sensor placement technique can tolerate
804 inconsistencies/inaccuracies which typically exist in the water utility hydraulic
805 models which have been used to determine the optimal sensor configurations.
- 806 • Results demonstrated that the system can typically locate leaks/bursts to a small
807 fraction of the DMA (best localisation performance achieved was approximately
808 14%). The framework was proven to be able to successfully locate leaks/bursts as
809 small as 3.5% of the peak daily flow with as few as 3 additional pressure sensors
810 installed.

811

812 **DATA AVAILABILITY STATEMENT**

813 Some or all data, models, or code generated or used during the study are proprietary or
814 confidential in nature and may only be provided with restrictions. Direct requests for these
815 materials may be made to the provider (United Utilities). The thesis underpinning this paper is
816 available for download (Boatwright, 2020).

817

818 **ACKNOWLEDGEMENTS**

819 The authors wish to thank the innovation team at United Utilities and the engineering and
820 physical sciences research council (EPSRC) for funding this work under a STREAM IDC
821 research project (grant number EP/L015412/1).

822

823

824 **REFERENCES**

825 Blesa, J., Nejjari, F. and Sarrate, R. (2016). Robust sensor placement for leak location:
826 analysis and design. *Journal of Hydroinformatics*, 18, 1, 136–148.

827 Boatwright, S., Romano, M., Mounce, S. R., Woodward, K. and Boxall, J. B. (2016).

828 Approximate location of leaks and bursts in a district metered area using statistical process

829 control and geostatistical techniques, Proc. 14th International Computing and Control for the

830 Water Industry Conference, Amsterdam, Netherlands.

831 Boatwright, Shaun (2020) Integrated optimal pressure sensor placement and localisation of

832 leak/burst events using interpolation and a genetic algorithm. EngD thesis, University of

833 Sheffield. <https://etheses.whiterose.ac.uk/29227/>

834 Casillas, M. V.; Garza-Castanon, L. E. and Puig, V. (2013a). Model-based leak detection and

835 location in water distribution networks considering an extended-horizon analysis of pressure

836 sensitivities. *Journal of Hydroinformatics*, 16, 3, 649–670.

837 Casillas, M. V., Puig, V., Garza-Castanon, L. E. and Rosich, A. (2013b). Optimal sensor

838 placement for leak location in water distribution networks using genetic algorithms. *Sensors*,

839 13, 11, 14984–15005.

840 Casillas, M. V., Garza-Castanon, L. E. and Puig, V. (2015). Optimal sensor placement for

841 leak location in water distribution networks using evolutionary algorithms”. *Water*, 7, 11,

842 6496–6515.

843 Colombo, A. F., Karney, B. W. (2002) Energy and costs of leaky pipes: toward

844 comprehensive picture. *J Water Resour Plan Manag* 128(6):441–450.

845 Daniel, I., Pesantez, J., Letzgus, S., Fasaee, M. A. K., Alghamdi, F., Berglund, E.,
846 Mahinthakumar, G. and Cominola, A. (2023) A Sequential Pressure-Based Algorithm for
847 Data-Driven Leakage Identification and Model-Based Localization in Water Distribution
848 Networks. *J. Water Resour. Plann. Manage.*, 2022, 148(6): 04022025 de Mesnard, L. (2013).
849 Pollution models and inverse distance weighting: Some critical remarks. *Computers and*
850 *Geosciences*. 52:459-469.

851 Farley, B., Mounce, S. R. and Boxall, J. B. (2013). Development and Field Validation of a
852 Burst Localization Methodology. *J Water Res. Plan. Man.* 139(6):604-13.

853 Fox, S., Shepherd, W., Collins, R. and Boxall, J. B. (2016). Experimental quantification of
854 contaminant ingress into a buried leaking pipe during transient events. *Journal of Hydraulic*
855 *Engineering*, 142 (1), 04015036.

856 Fuchs-Hanusch, D. and Steffelbauer, D. (2016). Real-world comparison of sensor placement
857 algorithms for leakage localisation. *Proceedings of the 18th Water Distribution Systems*
858 *Analysis Conference, Cartagena de Indias, Colombia.*

859 Huang, Y., Zheng, F., Kapelan, Z., Savic, D., Duan, H.-F., & Zhang, Q. (2020). Efficient leak
860 localization in water distribution systems using multistage optimal valve operations and smart
861 demand metering. *Water Resources Research*, 56, e2020WR028285.
862 <https://doi.org/10.1029/2020WR028285>.

863 Kapelan, Z., Savic, D. A. and Walters, G. A. (2005). “Optimal sampling design
864 methodologies for water distribution model calibration”. *Journal of Hydraulic Engineering*,
865 131, 3, 190–200.

866 Li, R., Huang, H., Xin, K. and Tao, T. (2015). A review of methods for burst/leakage
867 detection and location in water distribution systems. *Water Science & Technology: Water*
868 *Supply*, 15, 3, 429–441.

869 Marzola, I., Mazzoni, F., Alvisi, S. and Franchini, M. (2022). Leakage Detection and
870 Localization in a Water Distribution Network through Comparison of Observed and
871 Simulated Pressure Data. *J. Water Resour. Plann. Manage.*, 2022, 148(1): 04021096. DOI:
872 10.1061/(ASCE)WR.1943-5452.0001503

873 Mounce, S. R., Boxall, J. B. and Machell, J. (2010). Development and Verification of an
874 Online Artificial Intelligence System for Detection of Bursts and Other Abnormal Flows. *J.*
875 *Water Res. Plan. Man.* 136(3):309-18.

876 Mutikanga H. E., Sharma, S. K., Vairavamoorthy, K. (2013). Methods and tools for
877 managing losses in water distribution systems. *J Water Resour Plan Manag* 139(2):166–174.

878 Ostfeld, A. and Salomons, E. (2004). “Optimal layout of early warning detection stations for
879 water distribution systems security. *Journal of Water Resources Planning and Management*,
880 130, 5, 377–385.

881 Pérez, R., Puig, V., Pascual, J., Peralta, A., Landeros, E. and Jordanas, L. (2009). “Pressure
882 sensor distribution for leak detection in Barcelona water distribution network”. *Water Science*
883 *& Technology Water Supply*, 9, 6, 715–721.

884 Puust, R., Kapelan, Z., Savic, D. A. and Koppel, T. (2010) A review of methods for leakage
885 management in pipe networks,” *Urban Water J.*, vol. 7 (1), pp. 25-45, 2010.

886 Qi, Z., Zheng, F., Guo, D., Maier, H. R., Zhang, T., Yu, T. and Shao, Y. (2018a). Better
887 understanding of the capacity of pressure sensor systems to detect pipe burst within water
888 distribution networks. *J. Water Resour. Plann. Manage.*, 2018, 144(7): 04018035.

889 Qi, Z., Zheng, F., Guo, D., Zhang, T., Shao, Y., Yu, T., Zhang, K., & Maier, H. R. (2018b). A
890 comprehensive framework to evaluate hydraulic and water quality impacts of pipe breaks on
891 water distribution systems. *Water Resources Research*, 54, 8174–8195.
892 <https://doi.org/10.1029/2018WR022736>

893 Romano, M., Kapelan, Z. and Savic, D. A. (2013). Geostatistical Techniques for
894 Approximate Location of Pipe Burst Events in Water Distribution Systems, *J. Hydroinform.*
895 15(3):634–651.

896 Romano, M., Kapelan, Z. and Savic, D. A. (2014). Automated Detection of Pipe Bursts and
897 Other Events in Water Distribution Systems, *J. Water Res. Plan. Man.* 140(4):457-67.

898 Romano, M. (2020). Review of Techniques for Optimal Placement of Pressure and Flow
899 Sensors for Leak/Burst Detection and Localisation in Water Distribution Systems, in Dawei
900 H., Mounce, S., Scozzari, A., Soldovieri, F., and Solomatine, D. (eds.), *ICT for Smart Water*
901 *Systems: Measurements and Data Science*, Hdb Env Chem.

902 Romano, M., Boatwright, S., Mounce, S. R., Nikoloudi, E. and Kapelan, Z. (2020). AI- based
903 event management at United Utilities. *HydroLink, IAHR*. No. 4/2020, pp.104-108.

904 Sanz, G., Perez, R., Kapelan, Z. and Savic, D. (2016). Leak detection and localization
905 through demand components calibration. *J. Water Resour. Plann. Manage.*, 2016, 142(2):
906 04015057.

907 Shastri, Y. and Diwekar, U. (2006). Sensor placement in water networks: a stochastic
908 programming approach. *Journal of Water Resources Planning and Management*, 132, 3, 192–
909 203.

910 Soldevila, A., Blesa, J., Fernandez-Canti, R. M., Tornil-Sin, S. and Puig, V. (2019). Data-
911 Driven Approach for Leak Localization in Water Distribution Networks Using Pressure
912 Sensors and Spatial Interpolation. *Water*, 11(7):1500.

913 Sophocleous, S., Savić, D., & Kapelan, Z. (2019). Leak Localization in a Real Water
914 Distribution Network Based on Search-Space Reduction. *J. Water Res. Plan. Man.*
915 145(7):04019024.

916 Steffelbauer, D. and Fuchs-Hanusch, D. (2016). “Efficient sensor placement for leak
917 localization considering uncertainties”. *Water Resources Management*, 30, 14, 5517–5533.

918 Steffelbauer, D., Deuerlein, J., Gilbert, D., Abraham, E. and Piller, O. (2022). Pressure-Leak
919 duality for leak detection and localization in water distribution systems. *J. Water Resour.*
920 *Plann. Manage.*, 2022, 148(3): 04021106.

921 Wang, Q., Savic, D. A. and Kapelan, Z. (2017).
922 GALAXY: A new hybrid MOEA for the optimal design of Water Distribution systems,
923 *Water Resour. Res.* 53:1997-2015.

924 Wang, X., Guo, G., Liu, S., Wu, Y., Xu, X. and Smith, K. (2020). Burst detection in district
925 metering areas using deep learning method. *J. Water Resour. Plann. Manage.*, 2020, 146(6):
926 04020031.

927 Wu, Y. and Liu, S. (2017). A review of data-driven approaches for burst detection in water
928 distribution systems, *Urban Water Journal*, 14:9, 972-983, DOI:
929 10.1080/1573062X.2017.1279191

929 Wu, Y., Liu, S. and Wang, X. (2018). Distance-Based burst detection using multiple pressure
930 sensors in district metering areas. *J. Water Resour. Plann. Manage.*, 2018, 144(11):
931 06018009.

932 Xu, W., Zhou, X., Xin, K., Boxall, J., Yan, H., and Tao, T. (2020). Disturbance extraction for
933 burst detection in water distribution networks using pressure measurements. *Water Resources*
934 *Research*, 56, e2019WR025526. <https://doi.org/10.1029/2019WR025526>.

935 Zhang, Q., Zheng, F., Kapelan, Z., Savic, D., He, G. and Ma, Y. (2020). Assessing the global
936 resilience of water quality sensor placement strategies within water distribution systems.
937 *Water Research*, Volume 172, 2020, 115527, ISSN 0043-1354,
938 <https://doi.org/10.1016/j.watres.2020.115527>.

939 Zimmerman, D., Pelvic, C., Ruggles, A. and Armstrong, M. P. (1999). An Experimental
940 Comparison of Ordinary and Universal Kriging and Inverse Distance Weighting, *Math. Geol.*
941 31(4),375–390.

942

943 **Table 1:** Leak/burst event sizes and leak/burst event grouping results for the validation DMA

944

Leak/burst event size (emitter coefficient (l/s/m ^{0.5}))	Number of valid leak/burst event groups
0.1	3
0.2	437
0.3	469
0.4	18
0.5	4
0.6	2
0.7	1
Total	934

949

950 **Table 2:** Results for the optimal sensor configurations for the 16 engineered events in
 951 validation DMA (% of DMA search area). Events in bold were correctly localised

Engineered Event Number	Number of Optimal Sensors							
	3	4	5	6	7	8	9	10
1	38.7	33.2	36.2	61.2	61.2	61.1	61.3	61.3
2	30.7	29.5	30.7	9.5*	9.5*	15.4*	13.5*	0.8
3	23.4	20.8	23.4	2.4	2.4	9.9*	10.1*	14.4
4	39.4	22.1	35.5	6.2	6.1	14.3	15.6	18.4
5	30.7	65.9	25.1	20.9	20.9	17.6	18.7	11.9
6	28.6	28.4	25.1	2.4	2.4	2.4	2.4	2.4
7	28.6	28.9	25.1	8.6*	8.6*	5.6	5.8	5.8
8	23.4	31.5	18.5	23.3*	23.3*	18.0*	20.1*	14.2*
9	28.3	29.5	25.1	2.4	2.4	2.4	2.4	2.4
10	28.3	28.4	25.1	2.4	2.4	2.4	2.4	2.4
11	28.6	27.1	25.1	8.6*	8.6*	5.6	5.8	5.8
12	28.3	21.4*	35.5	20.9	20.9	39.7	39.9	31.1*
13	30.7	29.5	25.0	2.4	2.4	2.4	2.4	2.4
14	30.7	21.7	65.0	8.5*	6.1	8.1*	8.2*	8.2*
15	30.7	65.9	37.9	29.4*	29.4*	23.3*	26.9*	20.1*
16	54.3	29.5	43.6	28.9	28.6	23.4	23.5	20.4
Average Search Area	33.2	40.0	35.8	28.8	28.7	29.3	29.5	27.8
Correct Events	7	6	9	5	5	6	6	5
Events with multiple search areas	0	1	1	6	5	5	6	4
Equivalent objective function value	70.8	77.5	63.9	88.2	88.2	83.9	84.0	87.1

952

953